Estimations of Global Warming Potentials from Computational Chemistry Calculations for CH_2F_2 and Other Fluorinated Methyl Species Verified by Comparison to Experiment

Paul Blowers* and Kyle Hollingshead

Department of Chemical and Environmental Engineering, The University of Arizona, P.O. Box 210011, Tucson, Arizona 85721-0011

Received: December 30, 2008; Revised Manuscript Received: April 10, 2009

In this work, the global warming potential (GWP) of methylene fluoride (CH_2F_2), or HFC-32, is estimated through computational chemistry methods. We find our computational chemistry approach reproduces well all phenomena important for predicting global warming potentials. Geometries predicted using the B3LYP/6-311g** method were in good agreement with experiment, although some other computational methods performed slightly better. Frequencies needed for both partition function calculations in transition-state theory and infrared intensities needed for radiative forcing estimates agreed well with experiment compared to other computational methods. A modified CBS-RAD method used to obtain energies led to superior results to all other previous heat of reaction estimates and most barrier height calculations when the B3LYP/6-311g** optimized geometry was used as the base structure. Use of the small-curvature tunneling correction and a hindered rotor treatment where appropriate led to accurate reaction rate constants and radiative forcing estimates without requiring any experimental data. Atmospheric lifetimes from theory at 277 K were indistinguishable from experimental results, as were the final global warming potentials compared to experiment. This is the first time entirely computational methods have been applied to estimate a global warming potential for a chemical, and we have found the approach to be robust, inexpensive, and accurate compared to prior experimental results. This methodology was subsequently used to estimate GWPs for three additional species [methane (CH_4); fluoromethane (CH_3F), or HFC-41; and fluoroform (CHF_3), or HFC-23], where estimations also compare favorably to experimental values.

Introduction

Global warming is a scientifically based environmental impact incurred due to industrial, consumer, and natural processes. As awareness of global warming became apparent through the development of global warming potential (GWP) analyses, the Kyoto Protocol[1] was introduced and signed by nearly every industrialized country to control atmospheric emissions of six compounds or classes of compounds that contribute largely to planetary warming. The six compounds that are covered by the protocol are[2] CO_2, CH_4, N_2O, SF_6, hydrofluorocarbons (HFCs), and perfluorocarbons (PFCs). This paper will investigate in detail the GWP of methylene fluoride, also known as HFC-32, using quantum chemical methods, and will compare intermediate results and final GWPs to experimental data to demonstrate the viability of computational chemistry as a way of achieving accurate results. Summary comparisons for methane, fluoromethane, and fluoroform are also included to assess the robustness of the approach used in this work.

A general formula for GWP regarding trace gases is[3−5]

$$\mathrm{GWP}_i = \frac{\int_0^{\mathrm{TH}} a_i[x_i(t)]\,\mathrm{d}t}{\int_0^{\mathrm{TH}} a_{\mathrm{ref}}[x_{\mathrm{ref}}(t)]\,\mathrm{d}t} \quad (1)$$

where TH is the arbitrarily selected time horizon for the GWP the species will be considered over, a_i is the radiative forcing due to a unit increase in atmospheric concentration of species i, $[x_i(t)]$ is the time-dependent concentration of a pulse of species i, while the corresponding quantities for a reference gas are in the denominator. Typically, the TH is chosen to be 20, 100, or 500 years,[4,6] and the reference gas is chosen to be CO_2. GWP estimates for chemical species depend on the atmospheric lifetime of the compound released into the environment, the radiative forcing due to the absorption of energy in the 700−1500 cm^{-1} range,[7−9] and the time-dependent concentration of the species.[10] Figure 1a shows the information needed and the flow of information transformations to reach global warming potential estimates with experimental data.

The time-dependent concentrations of the species can be known through degradation reaction rates, adsorption rates onto particulates or solids, and absorption rates into liquids. Compared to degradation, the contribution of adsorption is small and will be assumed negligible in this work.[11] For nonaromatic saturated hydrocarbons like those studied in this work, the primary degradation mechanism is abstraction of a hydrogen atom via reaction with a hydroxyl radical. [12] The first part of the results section will focus on generating the kinetic parameters leading to accurate $x_i(t)$'s for the species through quantum mechanical determination of rate constants as a function of temperature.

Radiative forcing, a_i, can be found through experiments[4,13] or theory[14] and requires IR spectra and cross sections for the species of interest.[15] The second section of the results will demonstrate how to estimate this phenomenon, while the final section will present the theoretically predicted GWP.

Because carbon dioxide is often chosen as the reference gas, any change in the predicted CO_2 concentrations over the TH may lead to changes in the GWP_i. This is why some advocate

* To whom correspondence should be addressed. E-mail: blowers@engr.arizona.edu. Phone: 520-626-5319. Fax: 520-621-6048.

10.1021/jp8114918 CCC: $40.75
Published on Web 04/29/2009

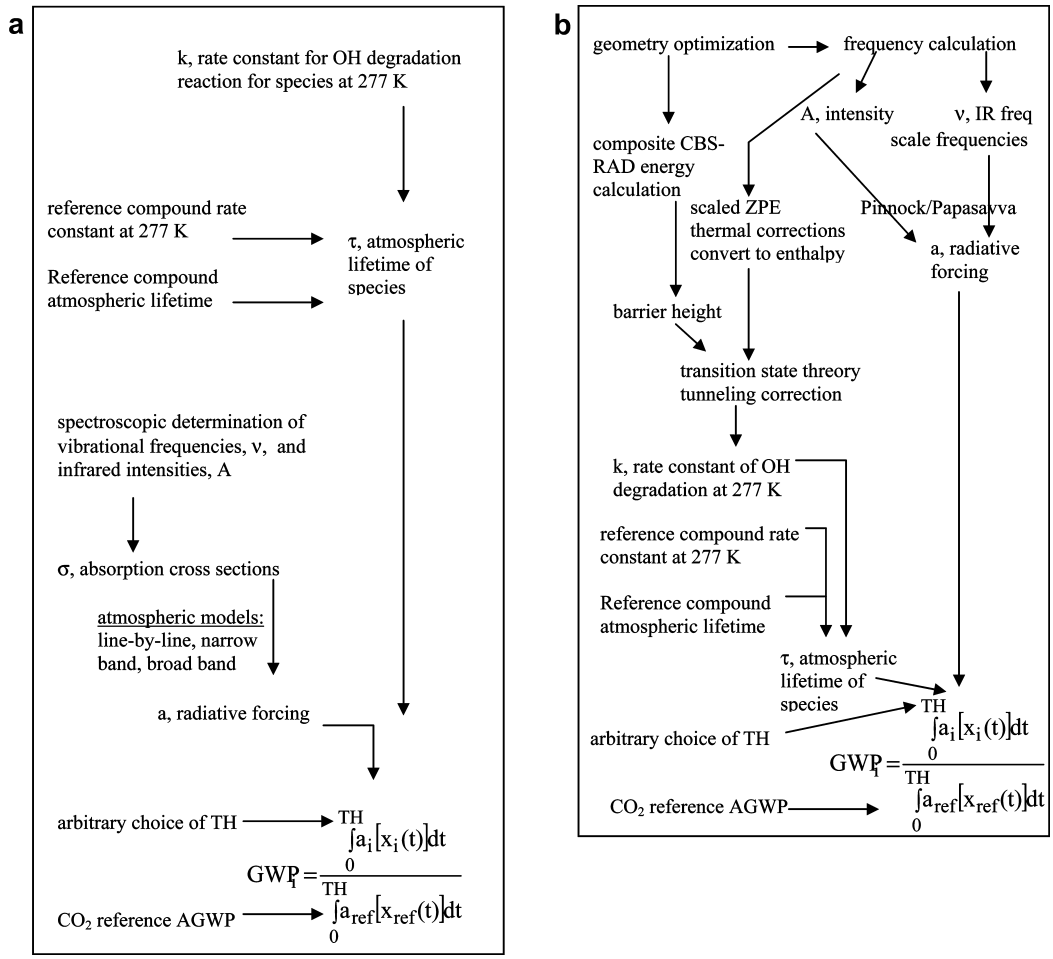

Figure 1. (a) Flow of information from experimental sources to reach global warming potential estimates. (b) Flow of information from purely computational chemistry methods to reach global warming potential estimates.

using only the numerator of the GWP_i as an assessment index instead of referencing it to CO_2, calling this the absolute GWP ($AGWP_i$). In this work, we will compute the numerator and use published CO_2 data to convert to GWP_i so comparisons can be made to prior results.[15]

GWPs are currently available for relatively few chemicals,[4] although estimates are continually being developed for new species. The small number of available GWPs is due to both the complexity of the kinetic experiments and the difficulties in making high-quality radiative forcing measurements through IR experiments.[9,15] Recent work is still populating databases regarding radiative forcing[16] of existing species while many of the newer CFC replacement materials have yet to be evaluated.[17] Additionally, differences in data among research groups for information going into the GWP estimation create the potential for large variations in GWP from one work to another.[15]

This work uses theoretical chemistry methods to predict global warming potentials in the absence of experimental data, as shown in Figure 1b. This is the first time that a complete series of calculations for GWP predictions using these methods has been done for any species, which highlights the utility of quantum chemical methods for obtaining high quality data when the necessary experiments are difficult or expensive to carry out.

Choice of Primary Species. Methylene fluoride is investigated at the primary species because there are data available at each intermediate step for comparison to demonstrate that quantum chemical methods can be robustly applied to predict all parts of global warming potential estimates.

Although CH_2F_2 is not listed on the U.S. Environmental Protection Agency (U.S. EPA) Toxic Release Inventory (TRI)[18] and emissions are difficult to estimate, this species has sufficient experimental data available to allow us to use the species as a benchmark species. It is true that other halogenated compounds are emitted into the atmosphere in higher quantities, like HFC-23 and HFC-134a;[19] however, CH_2F_2 is used as a replacement material for CFCs[20] and has an important commercial application as a fire extinguishant.[21,22] This use is noteworthy because the substance is chosen specifically to be emitted to the environment during its use. CH_2F_2 is also used as a refrigerant[23] and in the manufacture of other organic products.[24]

Expected Error Magnitudes. Several studies have been done on the kinetics of hydroxyl radical with CH_2F_2,[22,25−32] but there are little data available for comparison at the low temperatures encountered in the troposphere where degradation occurs. When work performed at lower temperatures was compared, discrepancies in experimental data also became larger.[33] Additionally, in the low temperature region, extrapolations of data from higher temperatures may fail because of non-Arrhenius curvature.[33] Kurylo and Orkin[33] and Wayne et al.[34] describe experimental difficulties encountered in measuring accurate rate constants for reactions of hydroxyl radicals with other species, and Kurylo and Orkin hypothesize that obtaining accurate ab initio results may be just as difficult as obtaining accurate experimental results and that analyses would require experimental data.[33] Contrary to their expectation, however, this work will show a direct application of robust quantum chemical methods to evaluate

kinetics and radiative forcing to render global warming potentials that are within typical experimental errors for this reaction.

Obtaining high quality IR spectra experimentally can be difficult, especially in the far-infrared region.[20] Experimental errors may originate from inadequate instrumental resolution,[35] sample (backward) emission, sample impurities,[16] temperature control, pressure measurements, path lengths, photometric errors, systematic equipment errors, and adsorption. While some of these errors can be minimized through experimental design, those that remain can still lead to experimental differences in integrated absorption coefficients of about 30%.[20]

Radiative forcings are available for relatively few species compared to the number of chemicals that are in industrial use, and for species where many values have been predicted like CH_2F_2 described above, there are discrepancies among the predictions. Experimental determination of radiative forcing involves uncertainties that include the assumed atmospheric composition, cloudiness, and sensitivity of the spectroscopic measurements.[36] A study of CF_3CH_2F using different atmospheric models with several sets of experimental cross sections found that even the best radiative forcing predictions would only agree to within 12−14%.[19,37] Other work suggests errors may be as much as 25%.[15] This shows that quantum chemical predictions that are within 14% of experimental data, at least for radiative forcing, are indistinguishable from experimentally based values.

There is some uncertainty in GWP because the CO_2 reference data are constantly being reevaluated and the original values used in each of the published works were not listed. We recommend that all GWP results using CO_2 as the reference species explicitly report the CO_2 reference data to allow comparisons among data sets.

Now that we have described the expected accuracy of experimental measurements to be used to validate our results at each step of the calculation, we will discuss the methodologies applied in this work.

Methods

Computational Chemistry. In this work, the Gaussian98 software package[38] was used to perform all quantum mechanical calculations, while the POLYRATE software package[39] was used to calculate tunneling coefficients and some components of the rate constants. The choice of computational method and basis set affects the quality of computational chemistry work. We have found[40−42] that the choice of basis set and method for the geometry optimization and frequency calculations is less important than the choice of energies used for rate constant estimation. Due to the lesser expense of density functional calculations and our past work reproducing experimental geometries, we used the B3LYP method combined with the 6-311g** basis set for geometry optimizations and frequency calculations. This is a slightly larger basis set than that of Lei's previous work on atmospheric chemistry reactions[43] where they used the 6-31g** basis set. A larger basis set was used by Liu[44] in their work on similar hydrogen abstraction reactions, but structures do not change significantly when larger basis sets are used.[45]

Several past papers used quantum chemical calculations to predict infrared intensities needed for radiative forcing estimates.[9] The inclusion of electron correlation is important for X−H band intensities for a host of smaller species,[9,46−49] which is why we selected the B3LYP method; it is one of the better DFT methods including a correlation function. Testing done by Hall and Schlegel found hybrid density functional methods were more accurate in reproducing IR intensities compared to high level calculations and experiment than HF, MP2, nonlocal, or gradient-corrected methods.[50] They also tested the effect of basis set choice on predicting IR intensities. As one moved from small basis sets to larger ones, 6-31g* had already captured most of the improvement possible compared to enlarging the basis set to 6-311+g(3df,3pd). Other work has shown that polarization is important as well,[46,48] which is why the 6-311g** basis set was chosen.

Smith et al.'s[23] work showed temperature did not significantly affect the integrated cross sections of the species, normally leading to changes of about 10% over a 100 deg change in temperature. Much of this change was due to a change in the overtone spectra, which already contribute little to the radiative forcing. Therefore, we use the infrared intensities and vibrational frequencies calculated at the default Gaussian98 temperature of 298.15 K.

All stable structures were verified to be stable structures through frequency calculations where minima had no negative eigenvalues and the first-order transition states had one negative eigenvalue corresponding to the reaction mode. An intrinsic reaction calculation was done on the adiabatic energy surface to ensure the transition states linked the correct reactants to products since complex energy surfaces can be difficult to investigate with just a frequency calculation. Frequencies were left unscaled because this basis set shows no need for scaling factors.[44]

Much of our work for radical species[40,51] has found that the CBS-RAD method[52] is reliable for heats of reaction and activation energies. This is because the large basis sets include polarization and the methods include correlation, which have both been found to be important for some halogenated species.[53] While other work on predicting halogenated organic reaction energetics[54] used the G2-(MP2,SVP) method, that method has not been validated to accurately predict activation energies. On the other hand, we have shown that a modified CBS-RAD[41,42] method reproduces barrier heights to within a few kilocalories/mole consistently. Also, this composite method should remove some of the errors associated with spin contamination found for similar reactions.[55]

In addition to using the high quality CBS-RAD composite energy method, zero point energies were included for all species.[56] For barrier heights, the change in the number of moles times the gas constant times the temperature was added to the internal energy results to convert to enthalpies.

Canonical Variational Transition-State Theory. Our reactions are bimolecular with low barriers to reaction, so rate constants are calculated using canonical variational transition-state theory with the following expressions:[57]

$$k^{GT}(T,s) = \frac{k_b T}{h} \kappa L \frac{Q_{TS}(s)}{N_a Q_{OH} Q_{CH_2F_2}} \exp\left(\frac{-V_{MEP}(s)}{RT}\right) \quad (2)$$

$$k^{CVT}(T) = \min_s k^{GT}(T,s) \quad (3)$$

where $Q_{CH_2F_2}$, Q_{OH}, and Q_{TS} are the complete translational−vibrational−rotational−electronic partition functions for the primary reactant and the transition state, respectively; L is the statistical factor, which is 4 for the CH_2F_2 reaction;[57] k_b is Boltzmann's constant; h is Plank's constant; N_a is Avogadro's number; $V_{MEP}(s)$ is the classical barrier height along the reaction coordinate; R is the ideal gas constant; and T is temperature in Kelvin. For the partition functions, we took into account the hindered rotor factors using the method of Pitzer and Gwinn,[58] computed by hand, and then included these factors as a

correction to the Polyrate results with no hindered rotors. Additionally, the partition function for the hydroxyl radical was handled with the treatment of Irikura to include degeneracy.[59]

Tunneling, κ, is a quantum effect where reactant molecules that do not classically have enough energy to cross the reaction barrier can sometimes react. Tunneling effects can be calculated with the Wigner correction[57] or the Eckart function at high temperatures, but both methods fail at lower temperatures.[60] Instead, we have chosen to use the small curvature tunneling method of Skodje[61] to predict tunneling at lower temperatures.

Radiative Forcing. Instantaneous radiative forcing has been defined as[13]

$$F_{\text{tot}} = \sum_{i=1}^{250} 10\sigma_i F(\upsilon_i) \tag{4}$$

where the spectra from 0 to 2500 cm^{-1} have been separated into 10 cm^{-1} bins, σ_i is the measured infrared (IR) cross section, and $F(\nu_i)$ is the radiative forcing for the species in that bin. While cross sections and radiative forcing functions can be found experimentally, they can also be obtained through quantum mechanical calculations. A simplification of the above formula leads to[14]

$$F_{\text{tot}} = \sum_{k} A_k F(\upsilon_k) \tag{5}$$

where A_k is the IR intensity evaluated for peak k. In ref 14, the MP2/6-31g** method and basis set yielded results that were within 3% of the complete method of Pinnock.[13] That work used the harmonic oscillator approach, which we will also use since the lower frequency results where hindered rotors are usually found will not change the results significantly. While overtone spectra and dipole moment functions can be calculated with ab initio methods,[62−68] these results appear to contribute less than 10% to the final GWP,[7,14,69] so this complexity was not included in this work.

In addition, Freckleton et al.[70] showed that moving from the extremely computationally demanding line-by-line method of radiative forcing evaluation to the narrow-band method used in this work would not lead to errors greater than 10%, even for species like CF_4 where this comparison would be most sensitive. Again, this is within the 14% error expected for even the highest quality model results. This justifies the use of the 10 cm^{-1} bin procedure we followed. While the atmospheric window between 700 and 1500 cm^{-1} [7−9] has been used extensively, research has shown that lower vibrational modes may also contribute to radiative forcing.[20] In this work, we expand the work of Elrod[10] and Papasavva[14] to encompass the lower frequency contributions down to 0 cm^{-1}.

Atmospheric Lifetime Estimation. Atmospheric lifetimes are found by multiplying the global atmospheric lifetime of a well-characterized reference compound, CH_3CCl_3, by the ratio of the OH reaction rate constant at 277 K for CH_3CCl_3 to that for a new species[71,72]

$$\tau_{\text{lifetime,R}} = \tau_{\text{lifetime,CH}_3\text{CCl}_3} \times \frac{k_{\text{OH+CH}_3\text{CCl}_3\text{(277K)}}}{k_{\text{OH+R(277K)}}} \tag{6}$$

The data from DeMore[73] et al. were used to estimate the rate constant of CH_3CCl_3 at 277 K to get a value of 6.686×10^{-15} cm^3/(molecule s).[71] While Kurylo and Orkin suggest a temperature of 272 K,[33] we will stick to the more common convention of 277 K. Because the reaction rate of species with the hydroxyl radical is dependent on the hydroxyl radical concentration, it is important to know that value to a high degree of accuracy. Unfortunately, analyses using many techniques give differences of 20−30% for the hydroxyl radical concentration,[33] which suggests that atmospheric lifetimes may have similar differences. The atmospheric lifetime of CH_3Cl_3 has been modeled to be 4.8 years,[74] but other work suggests it should be 5.9 years.[33] We will use a more recent value of 5.7 years in our work.[17]

Results and Discussion

Table S1 in the Supporting Information contains a comparison of geometry optimization data and different levels of theory compared to experimental geometries. Tables S2−S4 summarize geometry information and frequency predictions for the transition state and CHF_2. The geometries obtained at the B3LYP/6-311g** level of theory compare favorably to experimentally determined values.

Table S5a in the Supporting Information shows a summary of infrared peak locations from our predictions compared to experimental and other computational work. Peak locations, important to this research through eq 5, are predicted well at the chosen level of computation. It is not just the location of the vibrations that are important, but also the IR intensities must be accurate in order to predict radiative forcing correctly. The work of Kondo et al.[75] and others are compared with our work and earlier experiments in Table S5b in the Supporting Information. Direct comparison of calculated and experimental intensities is difficult due to overlap among some of the bands,[76] which is why some of the results in Table S5b have been combined. Infrared intensifies for CH_2F_2 from computation compare well to experimentally based values. Based on the comparisons shown in the Supporting Information, our choice of computational method and basis set is adequate.

Heat of Reaction. Reaction energetics and their accuracy are important through the barrier height in eq 2. One proxy measure of evaluating energies is to compare heats of reaction from predictions to experimentally based values. Heats of formation are readily available for CH_2F_2 (−107.71 kcal/mol), OH (9.319 kcal/mol), and H_2O (−57.799) in the NIST webbook.[77] However, the heat of formation for CHF_2 is not as readily available. Four results are available in the literature, and they are −57.1,[78] −55.7,[79] −58.6,[80] and −59.2[81] kcal/mol. In addition, computational work using the BAC-MP4 method suggests the heat of formation should be −59.11 kcal/mol,[82] with an uncertainty around 2 kcal/mol. The same methodology showed the heat of formation of CH_2F_2 would be −107.8 kcal/mol, which suggests this latter value may be most correct. Using an intermediate value of −57.65 kcal/mol for the CHF_2 radical heat of formation, we calculate an experimental heat of reaction of −17.06 kcal/mol. This is compared to the predicted results using the CBS-RAD method and B3LYP/6-311g** geometry optimization where we get a heat of reaction of −16.95 kcal/mol. Our error is only 0.11 kcal/mol.

Louis et al.[83] computed the heat of reaction at the PMP4-(SDTQ) level with the 6-311g(2d,2p) and 6-311++g(3df,3pd) basis sets and got results of −17.73 and −16.25 kcal/mol, respectively. El-Taher reported heats of reaction that ranged between −9.93 and −16.31 kcal/mol,[84] with several clustered near −16 kcal/mol using the highest levels of theory. The work of Korchowiec found a value of −18.4 kcal/mol.[85]

One can see that we obtain the best agreement with experimental values considering how large the differences are for the heat of formation of the CHF_2 radical. This demonstrates the CBS-RAD method performs well in estimating reaction energetics, as we have found before.[41,42,51]

TABLE 1: Comparison of Predicted Barrier Heights Compared to Experiment[a]

E_a (kcal/mol)	method
5.83	CBS-RAD//B3LYP/6-311g** (this work)
3.52	experimental[25]
3.10	experimental,[29 73]
27.44	UHF/3-21g*//UHF/3-21g*[86,b]
31.15	UHF/6-31g*[84]
2.19	MP2/3-21g*//UHF/3-21g*[86,b]
5.91	PMP2/6-31++g*//UHF/6-31g*[84]
6.07	G2/MP2(max) - no ZPE[22]
6.86	Eckart potential fit of G2 results[22]
2.1	B3LYP/6-311g(d,p)[87]
3.70	PMP4(SDTQ)/6-311g(3df,2p)//MP2/6-311g(2d,2p)[83]
3.56	PMP4(SDTQ)/6-311++g(3df,3pd)//MP2/6-311g(2d,2p)[83]
0.1	B3LYP/6-311g(2d,2p)[88]

[a] All barrier height results are compiled at 298.15 K to facilitate comparison due to the curvature in the log k versus $1/T$ plot. For computational results, all method listings are (energy level//geometry optimization level). [b] ZPE and thermal corrections included. Additionally, conversion to enthalpy from internal (electronic energy) was included, as in this work.

Barrier Height. A comparison of barrier height is not particularly useful[56] unless done at a single temperature where high quality data are available because of curvature in many of the hydroxyl hydrogen abstraction reaction kinetic plots. Table 1 shows a comparison of barrier heights at 298.15 K from a host of experimental and theoretical works.

The low barrier height of this reaction prevented some computational errors from becoming apparent in comparison to experiments, as errors tend to show up when the barriers get larger. For instance, MP2 is known to overestimate activation energies[88] but does not in this case. However, this overestimation is apparent with the HF results, which is also known to overpredict activation energies.[88] Likewise, DFT methods, including B3LYP, tend to give activation barriers that are too low.[88−91] On the basis of our experience, we hypothesize that these deviances only become apparent when activation energies are greater than about 15 kcal/mol, which is why the expected errors may not appear here.

The work of Louis et al.[83] gives results comparable in quality to the CBS-RAD results where their large basis set compensated for the lower level method. They also included thermal and zero-point energy corrections to obtain enthalpies, which most of the other works have not done. Their approach uses a large geometry optimization method and basis set with MP2/6-311g(2d,2p) calculations. We are interested in estimating GWPs for larger molecular systems so their approach would be too expensive for those species. All other barrier heights reported show poorer agreement compared to experimental values than our methodology, justifying our choice of basis set, method, and composite energy method.

The kinetic predictions in this work were used to compute an activation energy following the work of Garrett and Truhlar.[92] Using the instantaneous slope of ln k versus $1/T$ at room temperature yielded an activation energy of 3.51 kcal/mol, which is within 0.01 kcal/mol of the experimental value of Jeong and Kaufman[25] and 0.41 kcal/mol of the values from Hsu and Demore.[29,93] Prior computational work did not convert kinetic data to yield activation energies that can be compared to experiment. In this case, barrier heights are different from activation energies because low temperature tunneling effects are not included in the barrier height predictions. When tunneling effects are included, the resulting activation energy shows good agreement with experimental values.

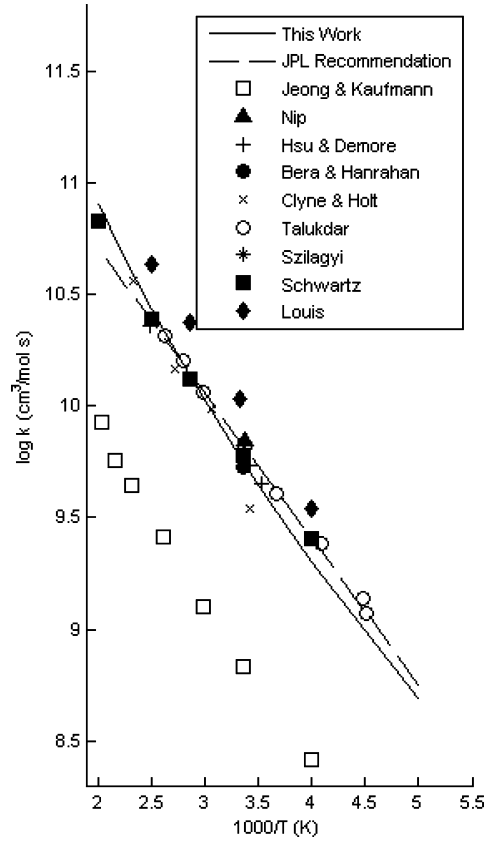

Figure 2. Comparison of rate constants for $CH_2F_2 + OH \rightarrow CHF_2 + H_2O$ predicted from theory at the CBS-RAD level using transition-state theory including tunneling corrections to experimental results. Here k is in units of cm^3/(mol s).[95,25,27,29,31,28,30,32,22,83]

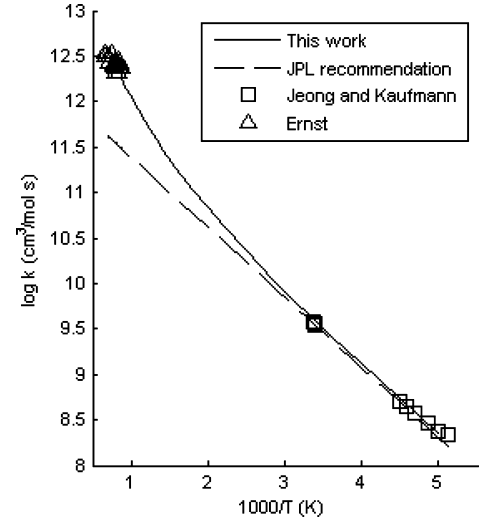

Figure 3. Rate constants for the $CH_4 + OH \rightarrow CH_3 + H_2O$ reaction where k is in units of cm^3 mol^{-1} s^{-1}.[95,25,102]

Rate Constants from Variational Transition-State Theory. A comparison of the current and past work to predict rate constants for the degradation of CH_2F_2 is shown in Figures 2 and 3. We see in Figure 2 that the experimental data from Jeong et al.[25] lie lower than any of the other results, while there are several sets of data that overlap about 1 order of magnitude higher. As discussed earlier, the experiments are challenging for these reactions as indicated by the order of magnitude difference.

Figure S1 (Supporting Information) compares past computational estimates of the rate constant; we see that our data lie

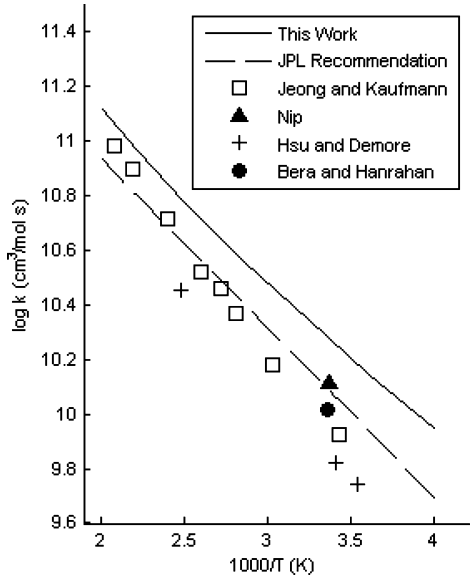

Figure 4. Rate constants for the $CH_3F + OH \rightarrow CH_2F + H_2O$ reaction where k is in units of $cm^3\ mol^{-1}\ s^{-1}$.[95,25,27,29,31]

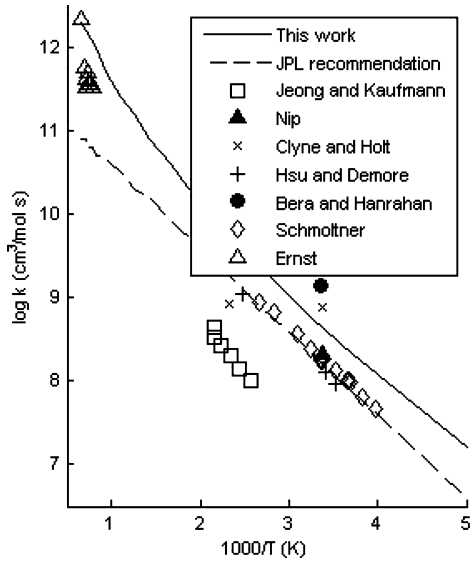

Figure 5. Rate constants for the $CHF_3 + OH \rightarrow CF_3 + H_2O$ reaction where k is in units of $cm^3\ mol^{-1}\ s^{-1}$.[95,25,102,27,29,31,28,103]

on top of the experimental data, and the text there supports a discussion with the result that our work is the first computational work that accurately predicts reaction rates for this reaction with no empirical fitting and no barrier shifting. We have now consistently found our methodology to work for a wide range of reactions.[40−42,94]

Our rate constants for the other fluorinated methyl species predicted from variational transition-state theory and Skodje et al.'s[61] small-curvature tunneling correction are compared to prior work in Figures 3, 4, and 5, and they agree well with experimental and other computational results for CH_4 and CH_3F. Our results for CHF_3 are about double the JPL recommended values,[95] still comparing favorably to experiment.

Atmospheric Lifetime. As discussed earlier, atmospheric lifetimes are important for differentiating the environmental impacts of chemicals. While the stratospheric lifetime of a species cannot be simplified as easily as the tropospheric lifetime, research has shown that the inclusion of stratospheric contributions is often a small correction to the tropospheric lifetime,[33] which is why we do not include stratospheric degradation in this work. The predicted kinetic rate through TST is 7.56×10^{-15} cm^3/(molecule s) at 277 K. The preferred value of 5.7 years for $\tau_{CH_3CF_3}$,[17] leads to an atmospheric lifetime of 6.20 years for our reaction of interest. This is compared to other published values in Table 2.

TABLE 2: Atmospheric Lifetimes in Years for All Investigated Species

source	CH_4	CH_3F	CH_2F_2	CHF_3
this work	8.67	1.64	6.20	88.22
Taylor et al.[a]	9.25			
Prather et al. full model[b]			6.8	
Prather et al. scaled results[b]			7.3	
ref 39 from Orkin et al.[c]			5.4	
Jain et al.[d]			5.6	
Wuebbles from WMO[e] and IPCC[f]			6.0	
Naik et al.[g]			5.4	234
Highwood et al.[h]				243
IPCC 2007[i]	12		4.9	270
calculated from JPL kinetics[j]	9.63	2.66	5.04	244

[a] Reference 96. [b] Reference 72. [c] Reference 97. [d] Reference 98. [e] Reference 99. [f] Reference 5 and 17. [g] Reference 17 [h] Reference 4. [i] Reference 100. [j] Reference 95.

Our lifetime for CH_4 of 8.68 years is shorter than the 9.25 years reported by Taylor et al.,[96] or the 12 years reported by the 2007 IPCC report[100] for CH_4. Our atmospheric lifetime of 6.20 years for CH_2F_2 is indistinguishable from the prior results, with values that vary from 4.9 years to 7.3 years, and is 0.3 years longer than the average of the other values. For CHF_3, our atmospheric lifetime is about a third of those reported by Naik et al.,[17] Highwood et al.,[4] and the IPCC report.[100] This error is attributable to the difference of our predicted rate constant for this species compared to prior work. No atmospheric lifetimes for CH_3F can be found for comparison, but our rate constant for CH_3F is within the acceptable margin of error compared to results estimated from JPL experimental kinetic data. Atmospheric lifetimes using the JPL recommended kinetic values for all species[95] are 9.63 years for CH_4, 2.66 years for CH_3F, 5.04 years for CH_2F_2, and 244 years for CHF_3. Our methodology is robust and leads to results that are similar to experimental ones.

Radiative Forcing Results. We turn to estimating radiative forcing using Pinnock's bin method, combined with Papasavva's ab initio transformation. Following the work of Papasavva,[69] we ignored the absorption overtone spectra because inclusion contributes a small percentage effect on the radiative forcing. In Table 3, we compare our predicted radiative forcing values to prior ones.

Our predicted radiative forcing value for CH_2F_2 is in very good agreement with the results of Pinnock et al.[13] and the WMO report,[99] with errors of 3% and 2%, respectively. Our poorest agreement occurs with the narrow-band model of Jain et al.,[98] where our value is 21% lower than theirs, and with the results of Highwood et al.[4] and the IPCC report,[100] where for both cases our value is 21% higher. Overall, our value of 0.133 W m^{-2} $ppbv^{-1}$ is 2.8% higher than the average of the other reported results, 0.1294 W m^{-2} $ppbv^{-1}$.

For methane, our methodology predicts a radiative forcing value between 25% and 40% lower than those reported by Jain et al.[98] and 200% higher than that presented in the 2007 Intergovernmental Panel on Climate Change report.[100] However, these values are small in magnitude, and a portion of the difference is likely due to rounding of results. The average of the other reported results is 0.0033 W m^{-2} $ppbv^{-1}$; our value of 0.003 W m^{-2} $ppbv^{-1}$ is 10% below this average.

For CH_3F, our predicted radiative forcing value agrees least with the value reported by Pinnock et al.,[13] where we under-

TABLE 3: Instantaneous Radiative Forcing Values in W m^{-2} $ppbv^{-1}$ and Relative Errors Compared to Each Available Experimental Data Point for All Investigated Species

source	CH_4	% error	CH_3F	% error	CH_2F_2	% error	CHF_3	% error
this work	0.003		0.024		0.133		0.183	
Jain et al., narrow band[a]	0.005	–25			0.168	–21	0.255	–28
Pinnock et al.[b]			0.032	–25	0.129	3	0.214	–14
Sihra et al.[c]			0.027	–11	0.114	17	0.117	56
WMO[d]			0.020	20	0.13	2	0.20	–9
Papasavva et al.[e]			0.026	–8	0.115	16	0.214	–14
Naik et al.[f]					0.148	–10	0.260	–30
Gohar et al.[g]					0.121	10	0.200	–9
Highwood et al.[h]					0.11	21	0.16	14
IPCC 2007[i]	0.004	–25			0.11	21	0.19	–4

[a] Reference 98. [b] Reference 13. [c] Reference 16. [d] Reference 99. [e] Reference 14. [f] Reference 17. [g] Reference 19. [h] Reference 4. [i] Reference 100.

TABLE 4: GWP Estimates for All Investigated Species at 20, 100, and 500 Year Time Horizons[a]

	CH_4			CH_3F		
source	GWP_{20}	GWP_{100}	GWP_{500}	GWP_{20}	GWP_{100}	GWP_{500}
this work	100	34	11	165	51	16
Jain et al.[b]	72	28	9			
IPCC 2007[d]	72	25	7.6			
this work (scaled)	80	27	9	132	41	13
Sihra et al.[e] (scaled)					160	
WMO[f] (scaled)	62	23	7	330	97	30

	CH_2F_2			CHF_3		
source	GWP_{20}	GWP_{100}	GWP_{500}	GWP_{20}	GWP_{100}	GWP_{500}
this work	2798	873	273	13935	14255	5855
Jain et al.[b]	3500	1100	350	15000	19600	15900
Naik et al.[c]	2920	889	276	15476	19691	15547
IPCC 2007[d]	2330	675	205	12000	14800	12200
this work (scaled)	2238	698	218	11148	11404	4684
Sihra et al.[e](scaled)		710			13000	
WMO[f] (scaled)	1800	550	170	9400	12000	10000

[a] Scaled GWPs are scaled following the method of Highwood and Shine.[4] [b] Reference 98. [c] Reference 17. [d] Reference 100. [e] Reference 16. [f] Reference 99.

predict by 25%, or with the value reported by the WMO,[99] where we overpredict by 20%. Our radiative forcing value is 8.6% below the average of the other reported results, 0.0263 W m^{-2} $ppbv^{-1}$.

For CHF_3, our result tends to be less than those reported by other research groups. Our best agreement is with the recent value used in the IPCC report,[100] where our value is 4% smaller. Our poorest agreements are with the work of Naik et al.,[17] where our value is smaller by 30%, and with the work of Sihra et al.,[16] where our value is larger by 56%. However, Sihra's value of 0.117 W m^{-2} $ppbv^{-1}$ is much smaller than the others reported. The average of the other reported results is 0.2066 W m^{-2} $ppbv^{-1}$ if Sihra's results are included or 0.2166 W m^{-2} $ppbv^{-1}$ if they are not included. Our value is 11.4 or 15.5% below these averages, respectively, which is still near the 14% expected minimum margin of error for radiative forcing measurements.[15]

Global Warming Potentials. The atmospheric lifetime can be combined with radiative forcing to obtain global warming potentials. Instead of using eq 1, we shift to the atmospheric lifetime based form to get[10]

$$\mathrm{GWP}_i = \frac{a_i \int_0^{\mathrm{TH}} e^{-t/\tau}\, dt}{\mathrm{AGWP}_{\mathrm{CO}_2}(\mathrm{TH})} \quad (7)$$

where we use the AGWPs at 20, 100, and 500 year time horizons for the CO_2 reference species previously introduced from Wuebble's work.[101]

If atmospheric lifetimes are longer than 200 years, one can use the radiative forcing directly to estimate GWP. However, Highwood and Shine[4] suggested scaling the radiative forcing by a multiplicative factor when atmospheric lifetimes are shorter. In our case, with an atmospheric lifetime less than 10 years for CH_2F_2, the radiative forcing was multiplied by 0.8 before performing the GWP calculation. However, not all previous work was scaled to the atmospheric lifetime. It should be noted that all GWPs have been scaled by an explicit comparison to the AGWP of CO_2, as discussed in the Introduction. While the AGWP of CO_2 may vary by up to 20% depending on the model used, we follow the work of Wuebbles and use AGWPs of CO_2 equal to 0.235, 0.768, and 2.459 (W year)/(m^2 ppmv) at TH's of 20, 100, and 500 years, respectively.[101] Table 4 summarizes our global warming prediction results.

For CH_2F_2, we predict a GWP of 2798 at 20 years, 873 at 100 years, and 273 at 500 years. If we use Highwood's method[4] of scaling for atmospheric lifetimes, we obtain 2238, 698, and 218 for these same time horizons, respectively. Pinnock's[13] results, which were not scaled for atmospheric lifetime, are in agreement with our unscaled results, with differences of less than 1.5% at each time horizon. Again, there have been no overall comparisons of how accurate GWPs are from one study to another. We would argue that, since the radiative forcing cannot be measured more accurately than within 14%,[37] GWPs also cannot be reproduced more accurately than that; we are

within that limit for CH_2F_2, even disregarding all other sources of experimental or computational errors.

Similar analyses show that we have an average error of 2.3% compared to Naik[17] and a 0.8% error compared to WMO values[99] at a 100 year time horizon. Orkin's work is a little more problematic as it introduces a new methodology and compares AGWP directly to CFC-11. We conclude from the magnitude of their numbers that they have actually computed a scaled result for atmospheric lifetime, although the details of their work are not clear. Jain's perceived overestimates of radiative forcing compared to other works suggest their GWP will be higher, and they are at all time horizons. Sihra reported a value only at 100 years, and their results were scaled by an atmospheric lifetime correction. We differ from their results by 1.7%.

Wuebble's results predate the introduction of atmospheric lifetime scaling for radiative forcing and come from two other compilations of data. It is unclear whether these were unscaled or scaled results, but the magnitudes suggest they were atmospheric lifetime scaled. Finally, Highwood and Shine[4] used scaled results that were higher than those of Wuebbles, and our error compared to those results is 11.5% on average.

Our calculated global warming potentials for other species are also compared with prior work in Table 4. We see that for methane, our unscaled predicted global warming potentials are somewhat higher than those from prior work at all time horizons. For CHF_3, our unscaled GWP is indistinguishable from the prior work over a 20 year time horizon, but over longer time horizons, we underpredict by increasingly larger factors, due largely to the difference between our predicted rate constants and other reported values. By scaling our results following the methods of Highwood and Shine,[4] we can also compare our work to other groups. For methane, our scaled results continue to be higher than those from the prior work at all time horizons. For CH_3F, our scaled results are lower than those from prior work at all time horizons. For CHF_3, our scaled results are indistinguishable from prior work at short time horizons but are substantially smaller at longer time horizons, again due to the factor of over prediction in our predicted rate constant.

In conclusion, with the possible exception of our kinetic predictions for the $CHF_3 + OH \rightarrow CF_3 + H_2O$ reaction, all of our intermediate values and final calculated GWPs are within acceptable ranges of accuracy compared to experimentally based values. The errors in our predicted radiative forcings for all species investigated are within expected margins of error for experimental measurements. Our predicted rate constants are within about 50% of experimental results for all but the $CHF_3 + OH \rightarrow CF_3 + H_2O$ reaction, which is in error by about a factor of 3. However, we believe that this error stems primarily from a difficulty encountered when using the CBS-RAD method to generate a reaction energy profile. We have investigated many species using the CBS-RAD method, and this is the only time our methodology has rendered poor results. We expect that using an alternative method and basis set to generate the reaction's energy profile will eliminate this error and recommend that multiple high-level methods and basis sets be compared to verify the accuracy of the rate constant when applying this methodology to a species where intermediate data is unavailable.

Conclusions

We find our computational chemistry approach accurately reproduces all phenomena important for predicting global warming potentials. Geometries using the B3LYP/6-311g** method were in good agreement with experiment. Frequencies needed for both partition functions in transition-state theory calculations and infrared intensities needed for radiative forcing estimates agreed well with experiment compared to other computational methods. The CBS-RAD energies used in this work were superior to other previous heat of reaction estimates and most barrier height calculations when the B3LYP/6-311g** optimized geometry was used as the base structure. The small-curvature tunneling correction and the hindered rotor approximation led to accurate reaction rate constants and radiative forcing estimates without requiring experimental data. Atmospheric lifetimes from theory at 277 K were indistinguishable from experimental results, as were the final global warming potentials compared to experiment. This is the first time complete ab initio methods have been applied to estimate global warming potentials for chemicals, and we have found the approach to be robust, inexpensive, and accurate compared to prior experimental results.

Supporting Information Available: This material includes in depth intermediate comparisons of geometry optimization, frequency, intensity, and other data compared to experimental data. The information also includes structures of all transition states to enable reproduction of this work if desired. This material is available free of charge via the Internet at http://pubs.acs.org.

References and Notes

(1) Kyoto protocol to the United Nations framework convention on climate change. In *United Nations*, 1998.

(2) United Nations Environment Programme: environment for development, 2005.

(3) Lashof, D. A.; Ahuja, D. R. *Nature (London, U.K.)* **1990**, *344*, 529.

(4) Highwood, E. J.; Shine, K. P. *J. Quant. Spectrosc. Radiat. Transfer* **2000**, *66*, 169.

(5) Houghton, J. T. *Climate change, 1994: radiative forcing of climate change and an evaluation of the IPCC IS92 emission scenarios*; University Press: New York, NY, 1995.

(6) Albritton, D. L. D. R. G.; Isaksen, I. S. A.; Lal, M.; Wuebbles, D. J. Trace Gas Radiative Forcing Indicies. In *Climate Change 1994*; Hougton, J. T., Meira Filho, L. G., Bruce, J., Lee, H., Callandar, B. A., Haites, E., Harris, N., Maskell, K. Eds.; Intergovernmental Panel on Climate Change, Press Syndicate of the University of Cambridge: New York, NY, 1995; 205 pp.

(7) Papasavva, S.; Illinger, K. H.; Kenny, J. E. *J. Phys. Chem.* **1996**, *100*, 10100.

(8) Sidebottom, H. W.; Franklin, J. *Pure Appl. Chem.* **1996**, *68*, 1757.

(9) Clerbaux, C.; Colin, R.; Simon, P. C.; Granier, C. *J. Geophys. Res.* **1993**, *98*, 10491.

(10) Elrod, M. J. *J. Chem. Educ.* **1999**, *76*, 1702.

(11) Khalil, M. A. K.; Rasmussen, R. A. *Environ. Sci. Pollut. Res.* **2000**, *7*, 79.

(12) Atkinson, R. *Chem. Rev.* **1985**, *85*, 69.

(13) Pinnock, S.; Hurley, M. D.; Shine, K. P.; Wallington, T. J.; Smyth, T. J. *J. Geophys. Res., [Atmos.]* **1995**, *100*, 23227.

(14) Papasavva, S.; Tai, S.; Illinger, K. H.; Kenny, J. E. *J. Geophys. Res.* **1997**, *102*, 13643.

(15) Fuglestvedt, J. S.; Berntsen, T. K.; Godal, O.; Sausen, R.; Shine, K. P.; Skodvin, T. *Clim. Change* **2003**, *58*, 267.

(16) Sihra, K.; Hurley, M. D.; Shine, K. P.; Wallington, T. J. *J. Geophys. Res., [Atmos.]* **2001**, *106*, 20493.

(17) Naik, V.; Jain, A. K.; Patten, K. O.; Wuebbles, D. J. *J. Geophys. Res.* **2000**, *105*, 6903.

(18) U.S. Environmental Protection Agency, Toxic Release Inventory, 2005.

(19) Gohar, L. K.; Myhre, G.; Shine, K. P. *J. Geophys. Res., [Atmos.]* **2004**, *109*, D01107.

(20) Beukes, J. A.; Niclaisen, F. M. *J. Quant. Spectrosc. Radiat. Transfer* **2000**, *66*, 185.

(21) *Kirk-Othmer Concise Encyclopedia of Chemical Technology*, 4th ed.; John Wiley & Sons, Inc.: New York, NY, 1999.

(22) Schwartz, M.; Marshall, P.; Berry, R. J.; Ehlers, C. J.; Petersson, G. A. *J. Phys. Chem. A* **1998**, *102*, 10074.

(23) Smith, K.; Newnham, D.; Page, M.; Ballard, J.; Duxbury, G. *J. Quant. Spectrosc. Radiat. Transfer* **1996**, *56*, 73.

(24) Hydrofluorocarbons (HFC), difluoromethane HFC-32.
(25) Jeong, K.-M.; Kaufman, F. *J. Phys. Chem.* **1982**, *86*, 1808.
(26) Howard, C. J.; Evenson, K. M. *J. Chem. Phys.* **1976**, *64*, 197.
(27) Nip, W. S.; Singleton, D. L.; Overend, R.; Paraskevopoulos, G. *J. Phys. Chem.* **1979**, *83*, 2440.
(28) Clyne, M. A.; Holtz, P. M. *J. Chem. Soc., Faraday Trans. 2* **1979**, *75*, 582.
(29) Hsu, K.-J.; DeMore, W. B. *J. Phys. Chem.* **1995**, *99*, 1235.
(30) Talukdar, R.; Mellouki, A.; Gierczak, T.; Burkholder, J. B.; McKeen, S. A.; Ravishankara, A. R. *J. Phys. Chem.* **1991**, *95*, 5815.
(31) Bera, R. K.; Hanrahan, R. J. *Radiat. Phys. Chem.* **1988**, *32*, 579.
(32) Szilagyi, I.; Dobe, S.; Berces, T. *React. Kinet. Catal. Lett.* **2000**, *70*, 319.
(33) Kurylo, M. J.; Orkin, V. L. *Chem. Rev.* **2003**, *103*, 5049.
(34) Wayne, R. P.; Canosa-Mas, C. E.; Heard, A. C.; Parr, A. D. *Atmos. Environ.* **1992**, *26A*, 2371.
(35) Orkin, V. L.; Guschin, A. G.; Larin, I. K.; Huie, R. E.; Kurylo, M. J. *J. Photochem. Photobiol., A: Chem.* **2003**, *157*, 211.
(36) Pinnock, S.; Shine, K. P. *J. Atmos. Sci.* **1998**, *55*, 1950.
(37) Forster, P. M. d. F.; Burkholder, J. B.; Clerbaux, C.; Coheur, P. F.; Dutta, M.; Gohar, L. K.; Hurley, M. D.; Myhre, G.; Portman, R. W.; Shine, K. P.; Wallington, T. J.; Wuebbles, D. *J. Quant. Spectrosc. Radiat. Transfer* **2005**, *93*, 447.
(38) Frisch, M. J.; Trucks, G. W.; Schlegel, H. B.; Scuseria, G. E.; Robb, M. A.; Cheeseman, J. R.; Montgomery, J. A., Jr.; Vreven, T. Kudin, K. N. Burant, J. C.; Millam, J. M.; Iyengar, S. S.; Tomasi, J.; Barone, V.; Mennucci, B.; Cossi, M.; Scalmani, G.; Rega, N.; Petersson, G. A.; Nakatsuji, H.; Hada, M.; Ehara, M.; Toyota, K.; Fukuda, R.; Hasegawa, J.; Ishida, M.; Nakajima, T.; Honda, Y.; Kitao, O.; Nakai, H.; Klene, M.; Li, X.; Knox, J. E.; Hratchian, H. P.; Cross, J. B.; Bakken, V.; Adamo, C.; Jaramillo, J.; Gomperts, R.; Stratmann, R. E.; Yazyev, O.; Austin, A. J.; Cammi, R.; Pomelli, C.; Ochterski, J. W.; Ayala, P. Y.; Morokuma, K.; Voth, G. A.; Salvador, P.; Dannenberg, J. J.; Zakrzewski, V. G.; Dapprich, S.; Daniels, A. D.; Strain, M. C.; Farkas, O.; Malick, D. K.; Rabuck, A. D.; Raghavachari, K.; Foresman, J. B.; Ortiz, J. V.; Cui, Q.; Baboul, A. G.; Clifford, S.; Cioslowski, J.; Stefanov, B. B.; Liu, G.; Liashenko, A.; Piskorz, P.; Komaromi, I.; Martin, R. L.; Fox, D. J.; Keith, T.; Al-Laham, M. A.; Peng, C. Y.; Nanayakkara, A.; Challacombe, M.; Gill, P. M. W.; Johnson, B.; Chen, W.; Wong, M. W. ; Gonzalez, C.; Pople, J. A. *Gaussian03*, Revision C.02; Gaussian, Inc.: Wallingford, CT, 2004.
(39) Corchado, J. C.; Chuang, Y.-Y.; Fast, P. L.; Hu, W.-P.; Liu, X.-P.; Lynch, G. C.; Nguyen, K. A.; Jackels, C. F.; Fernandez Ramos, A.; Ellingson, B. A.; Lynch, B. J.; Zheng, J.; Melissas, V. S.; Villa, J.; Rossi, I.; Coitino, E. L.; Pu, J.; Albu, V.; Steckler, R.; Garrett, B. C.; Isaacson, A. D.; Truhlar, D. G. *POLYRATE*, version 9.7; University of Minnesota: Minneapolis, MN, 2007.
(40) Blowers, P.; Zheng, X.; Zhang, N. *Mol. Simul.* **2005**, *31*, 615.
(41) Zheng, X.; Blowers, P. *J. Mol. Catal. A* **2006**, *246*, 1−10.
(42) Zheng, X.; Blowers, P. *Mol. Simul.* **2005**, *31*, 615.
(43) Lei, W.; Zhang, R.; Molina, L. T.; Molina, M. J. *J. Phys. Chem. A* **2002**, *106*, 6415.
(44) Liu, J.-y.; Li, Z.-s.; Dai, Z.-w.; Huang, X.-r.; Sun, C.-c. *Chem. Phys. Lett.* **2002**, *362*, 39.
(45) Perez-Casany, M. P.; Sanchez,-Marin, J.; Nebot-Gil, I. *J. Am. Chem. Soc.* **2000**, *122*, 11585.
(46) Yamaguchi, Y.; Frisch, M.; Gaw, J.; Schaefer, H. F., III; Binkley, J. S. *J. Chem. Phys.* **1986**, *84*, 2262.
(47) Miller, M. D.; Jensen, F.; Chapman, O. L.; Houk, K. N. *J. Phys. Chem.* **1989**, *93*, 4495.
(48) Bruns, R. E.; Guadagnini, P. H.; Scarminio, I. S.; de Barros Neto, B. *J. Mol. Struct.: THEOCHEM* **1997**, *394*, 197.
(49) Amos, R. D.; Handy, N. C.; Green, W. H.; Jayatilaka, D.; Willetts, A.; Palmieri, P. *J. Chem. Phys.* **1991**, *95*, 8323.
(50) Halls, M. D.; Schlegel, H. B. *J. Chem. Phys.* **1998**, *109*, 10587.
(51) Blowers, P.; Zheng, X.; Homan, K. *Chem. Eng. Commun.* **2003**, *190*, 1233.
(52) Mayer, P. M.; Parkinson, C. J.; Smith, D. M.; Radom, L. *J. Chem. Phys.* **1998**, *108*, 604.
(53) da Silva, J. B. P. *J. Braz. Chem. Soc.* **2000**, *11*, 219.
(54) Hou, H.; Wang, B.; Gu, Y. *J. Phys. Chem. A* **2000**, *104*, 1570.
(55) Kharroubi, M.; de Sainte Claire, P. *J. Phys. Chem. A* **2003**, *107*, 4483.
(56) Pacey, P. D. *J. Chem. Educ.* **1981**, *58*, 612.
(57) Duncan, W. T.; Bell, R. L.; Truong, T. N. *J. Comput. Chem.* **1998**, *19*, 1039.
(58) Pitzer, K. S.; Gwinn, W. D. *J. Chem. Phys.* **1942**, *10*, 428.
(59) Irikura, K. K.; Fruruip, D. J. *Computational thermochemistry: Prediction and estimation of molecular thermodynamics*; American Chemical Society: Washington, DC, 1998.
(60) Gonzalez-Lafont, A.; Lluch, J. M.; Espinosa-Garcia, J. *J. Phys. Chem. A* **2001**, *105*, 10553.
(61) Skodje, R. T.; Truhlar, D. G.; Garrett, B. C. *J. Phys. Chem.* **1981**, *85*, 3019.
(62) Lin, H.; Burger, H.; Mkadmi, E. B.; He, S.-G.; Yuan, L.-F.; Breidung, J.; Thiel, W.; Huet, T. R.; Demaison, J. *J. Chem. Phys.* **2001**, *115*, 1378.
(63) Espinosa-Garcia, J. *J. Phys. Chem. A* **2002**, *106*, 5686.
(64) Martell, J. M.; Boyd, R. J. *J. Phys. Chem.* **1995**, *99*, 13402.
(65) Daub, C. D.; Henry, B. R.; Sage, M. L.; Kjaergaard, H. G. *Can. J. Chem.* **1999**, *77*, 1775.
(66) He, S.-G.; Zheng, J.-J.; Hu, S.-M.; Lin, H.; Ding, Y.; Wang, X.-H.; Zhu, Q.-S. *J. Chem. Phys.* **2001**, *114*, 7018.
(67) Henry, B. R.; Kjaergaard, H. G. *Can. J. Chem.* **2002**, *80*, 1635.
(68) Takahashi, K.; Sugawara, M.; Yabushita, S. *J. Phys. Chem. A* **2002**, *106*, 2676.
(69) Papasavva, S.; Tai, S.; Esslinger, A.; Illinger, K. H.; Kenny, J. E. *J. Phys. Chem.* **1995**, *99*, 3438.
(70) Freckleton, R. S.; Pinnock, S.; Shine, K. P. *J. Quant. Spectrosc. Radiat. Transfer* **1996**, *55*, 763.
(71) Patten, K. O., Jr.; Li, Z.; Wuebbles, D. J. *J. Geophys. Res.* **2000**, *105*, 11625.
(72) Prather, M.; Spivakovsky, C. M. *J. Geophys. Res., [Atmos.]* **1990**, *95*, 18723.
(73) DeMore, W. B. *J. Phys. Chem.* **1996**, *100*, 5813.
(74) Prinn, R. G.; Weiss, R. F.; Miller, B. R.; Huang, J.; Alyea, F. N.; Cunnold, D. M.; Fraser, P. J.; Hartley, D. E.; Simmonds, P. E. *Science* **1995**, *269*, 187.
(75) Kondo, S.; Nakanaga, T.; Saeki, S. *J. Chem. Phys.* **1980**, *73*, 5409.
(76) Fox, G. L.; Schelegel, H. B. *J. Chem. Phys.* **1990**, *92*, 4351.
(77) Afeefy, H. F.; Liebman, J. F.; Stein, S. E. Neutral Thermochemical Data. In *NIST Chemistry WebBook, NIST Standard Reference Database Number 69*; Mallard, E. P. J. L. a. W. G. Ed.; National Institute of Standards and Technology: Gaithersburg MD, 2005.
(78) Pickard, J. M.; Rodgers, A. S. *Int. J. Chem. Kinet.* **1983**, *15*, 569.
(79) Luke, B. T.; Loew, G. H.; McLean, A. D. *J. Am. Chem. Soc.* **1987**, *109*, 1307.
(80) Lee, E. P. F.; Dyke, J. M.; Mayhew, C. A. *J. Phys. Chem. A* **1998**, *102*, 8349.
(81) McMillen, D. F.; Golden, D. M. *Annu. Rev. Phys. Chem.* **1982**, *33*, 493.
(82) Zachariah, M. R.; Westmoreland, P. R.; Burgess, D. R., Jr.; Tsang, W.; Melius, C. F. *J. Phys. Chem.* **1996**, *100*, 8737.
(83) Louis, F.; Gonzalez, C. A.; Huie, R. E.; Kurylo, M. J. *J. Phys. Chem. A* **2000**, *104*, 8773.
(84) El-Taher, S. *Int. J. Quantum Chem.* **2001**, *84*, 426.
(85) Korchowiec, J.; Kawahara, S.; Matsumura, K.; Uchimaru, T.; Sugie, M. *J. Phys. Chem. A* **1999**, *103*, 3548.
(86) Bottoni, A.; Poggi, G.; Emmi, S. S. *J. Mol. Struct.: THEOCHEM* **1993**, *279*, 299.
(87) Korchowiec, J. *J. Phys. Org. Chem.* **2002**, *15*, 524.
(88) Jursic, B. S. *Chem. Phys. Lett.* **1996**, *256*, 603.
(89) Yamataka, H.; Nagase, S.; Ando, T.; Hanafusa, T. *J. Am. Chem. Soc.* **1986**, *108*, 601.
(90) Lee, W. T.; Masel, R. I. *J. Phys. Chem.* **1996**, *100*, 10945.
(91) Lee, W. T.; Masel, R. I. *J. Phys. Chem.* **1995**, *99*, 9363.
(92) Garrett, B. C.; Truhlar, D. G. *J. Am. Chem. Soc.* **1979**, *101*, 4534.
(93) Hsu, K.-J.; DeMore, W. B. *J. Phys. Chem.* **1995**, *99*, 11141.
(94) Zheng, X.; Blowers, P. *J. Mol. Catal. A: Chem.* **2005**, *242*, 18−25.
(95) Sander, S. P.; Friedl, R. R.; Ravishankara, A. R.; Golden, D. M.; Kolb, C. E.; Kurylo, M. J.; Huie, R. E.; Orkin, V. L.; Molina, M. J.; Moortgat, G. K.; Finlayson-Pitts, B. J. *Chemical kinetics and photochemical data for use in atmospheric studies*; Jet Propulsion Laboratory and California Institute of Technology: Pasadena, CA, 2003.
(96) Taylor, J. A. B. G. P.; Zimmerman, P. R.; Cicerone, R. J. *J. Geophys. Res.* **1991**, *96*, 3013.
(97) Orkin, V. L.; Khamaganov, V. G.; Guschin, A. G.; Huie, R. E.; Kurylo; M. J. *International Symposium on Gas Kinetics*; University College Dublin: Dublin, Ireland, 1994.
(98) Jain, A. K.; Briegleb, B. P.; Minschewaner, K.; Wuebbles, D. J. *J. Geophys. Res., [Atmos.]* **2000**, *105*, 20773.
(99) WMO Scientific Assessment of Ozone Depletion. World Meteorological Organisation, 1999.
(100) Solomon, S.; Qin, D.; Manning, M.; Chen, Z.; Marquis, M.; Averyt, K. B.; Tignor, M.; Miller, H. L. *IPCC, 2007; Climate Change 2007: The Physical Science Basis. Contribution of Working Group I to the Fourth Assessment Report for the Intergovernmental Panel on Climate Change*, Cambridge University Press: Cambridge, U.K., 2007.
(101) Wuebbles, D. J. *Annu. Rev. Energy Environ.* **1995**, *20*, 45.
(102) Ernst, J. W. H. G.; Zellner, R. *Ber. Bunsen−Ges. Phys. Chem.* **1978**, *82*, 409.
(103) Schmoltner, A. M.; Talukdar, R. K.; Warren, R. F.; Mellouki, A.; Goldfarb, L.; Gierczak, T.; McKeen, S. A.; Ravishankara, A. R. *J. Phys. Chem.* **1993**, *97*, 8976.

JP8114918